Supporting information for:

Potential uses of coal methane in China and associated benefits for air quality, health, and climate

Mingyang Zhang[†], Sarah M. Jordaan[‡], Wei Peng[§], Qiang Zhang[‖], Scot M. Miller[†]*

†Department of Environmental Health and Engineering, Johns Hopkins University, Baltimore, MD, USA.

‡School of Advanced International Studies, Johns Hopkins University, Washington, DC, USA.

§School of International Affairs and Department of Civil and Environmental Engineering, Pennsylvania State University, State College, PA, USA.

‖Ministry of Education Key Laboratory for Earth System Modeling, Center for Earth System Science, Tsinghua University, Beijing, China.

Corresponding Author:

*Mingyang Zhang, Phone: 410-516-7095; fax: 410-516-8996; e-mail: mzhang78@jhu.edu

Number of pages: 19 (including the cover page)

Number of figures: 5

Number of tables: 4

S1 Coal mine methane emissions in China's 13 northern provinces

Table S1. Potential CBM/CMM by province (unit: Tg/yr).

The table below lists the utilization goals for coalbed methane (CBM) and coal mine methane (CMM) for the 8 provinces considered in this study.

Province	2020FYP		2020NEA	
	CBM	CMM	CBM	CMM
Shanxi	5	3	10.8	5.4
Henan	0.07	0.2	0.1	0.2
Anhui	0.07	0.4	-	0.4
Heilongjiang	0.07	-	-	-
Liaoning	0.07	-	0.1	-
Shaanxi	-	0.1	1.1	0.1
Inner-Mongolia	-	0.1	1.1	0.1
Gansu	-	0.1	-	0.1
Total in the 8 northern provinces	5.28	3.9	13.2	6.3
National goals	6	4.67	13.3	8

S2 Detailed calculation in the CBM/CMM scenarios

S2.1 Definition and data source of all variables

Note: Table S2 lists the specific data sources for the variables defined below.

Emissions factors:

EF_{coal}: CO_2 emission factor in coal power generation

EF_{NG}: CO_2 emission factor in natural gas power generation

EC_{coal}: CO_2 emission coefficients of coal combustion

EC_{NG}: CO_2 emission coefficients of natural gas combustion

GWP_{100}: 100-year global warming potential of methane

Heat content and Heat rate by fuel:

HC_{coal_pow}: Heat content of coal in power generation

HC_{coal_res}: Heat content of coal combustion

HC_{NG_res}: Heat content of natural gas in residential combustion

HC_{NG_pow}: Gas heat content of natural gas in power generation

HR_{coal}: Heat rate of coal in power generation

HR_{NG}: Heat rate of natural gas in power generation

ρ_{CH4}: NG density at standard temperature and pressure (0ºC and 1 atm)

Efficiency:

η_{gas}: Heat generation efficiency of the gas stove

η_{coal}: Heat generation efficiency of the household coal stove

$\eta_{electric}$: Heat generation efficiency of the electricity resistance heaters

$\rho_{T\&D\ loss}$: Transmission and distribution system electricity loss

R: Nature gas transmission leakage rate

Other variables defined in Equation (1)-(10):

CD_{POW}: Potential coal displacement in POW scenario (unit: kg)

$CD_{RES\text{-}GAS}$: Potential coal displacement in RES-GAS scenario (unit: kg)

$CD_{RES\text{-}ELEC}$: Potential coal displacement in RES-ELEC scenario (unit: kg)

CBM_i: Total coalbed methane in each province *i* (unit: bcm)

CMM_i: Total coal mine methane emissions in each province *i* (unit: bcm)

$Elec_i$: Potential electricity generation from CBM/CMM in each province *i* (unit: kwh)

$Heat_i$: Potential heat supply from CBM/CMM in each province *i* (unit: MMBtu)

$\Delta\ GHG_j$: Total reduced GHG emissions from CMM utilization scenario *j* (unit: Mt CO_2eq/yr)

$\Delta\ Carbon_j$: Reduced carbon dioxide emissions from scenario *j* compare to the base case (unit: Mt/yr)

$EF_{eff,i}$: Effective emission factor for coal-fired electricity in model grid box *i*

$E_{SO2,i}$: SO_2 emissions from coal-fired electricity generation in model grid box *i*

$E_{CO2,i}$: CO_2 emissions from coal-fired electricity generation in model grid box *i*

$E_{Nox,i}$: NOx emissions from coal-fired electricity generation in model grid box *i*

Table S2. Summary of data sources for emissions factors, heat content, and efficiency.

Category	Name	VALUE	Unit	References
Emissions Factors	EF_{coal}	0.86	kg (CO_2)/kwh	[1]
	EF_{NG}	0.46	kg (CO_2)/kwh	
	EC_{coal}	95.35	kg (CO_2)/MMBtu	[2]
	EC_{NG}	53.07	kg (CO_2)/MMBtu	
	GWP_{100}	32	$1CH_4$=$32CO_2$eq	[3]
Heat content and Heat rate by fuel	HC_{coal_res}	21610	Btu/kg	[4]
	HC_{coal_pow}	14959	Btu/kg	
	HC_{NG_pow}	36100	Btu/m^3	
	HC_{NG_res}	36100	Btu/m^3	
	HR_{NG}	8578	Btu/kwh	[5]
	HR_{coal}	10514	Btu/kwh	
	ρ_{CH4}	0.72	kg/m^3	[6]
Efficiency	$\eta_{electric}$	97%	%	[7]
	η_{gas}	83%	%	
	η_{coal}	69%	%	
Transport efficiency & Leakage	$\rho_{T\&D\ Loss}$	93%	%	[8]
	R	3%	%	[4]

S2.2 Potential electricity generation and heat supply from CBM/CMM in each province

We use Equation (1) to estimate potential electricity generation and Equation (2) to estimate the potential heat supply (see Sect. S3.1 for variable definitions and Table S2 for data sources):

$$Elec_i = CMM_i(1-R) \times HC_{NG_{pow}} / HR_{NG} + CBM_i(1-R) \times HC_{NG_{pow}} / HR_{NG} \quad (1)$$

$$Heat_i = CMM_i(1-R) \times HC_{NG\_res}/10^6 + CBM_i(1-R) \times HC_{NG\_res}/10^6 \quad (2)$$

S2.3 GHG emission reduction and coal displacement in each scenario

We use Equation (3) to estimate the total GHG emission changes and Equation (4)-(9) to estimate the carbon dioxide emission changes:

$$\Delta GHG_j = \sum_i CMM_i(1-R) \times \rho_{NG} \times GWP_{100} + \Delta Carbon_j \quad (3)$$

POW scenario: This carbon dioxide reduction occurs when coal is replaced by more efficient natural gas electricity generation.

$$CD_{POW} = \sum_i Elec_i \times HR_{coal}/HC_{coal\_pow} \quad (4)$$

$$\Delta Carbon_{POW} = (EF_{coal} - EF_{NG}) \times \sum_i Elec_i/10^9 \quad (5)$$

RES-GAS scenario: We replace small household coal stoves with gas stoves, and carbon dioxide emissions decline because these gas stoves are more efficient.

$$CD_{RES\_GAS} = \frac{\sum_i Heat_i \times \eta_{gas}}{\eta_{coal} \times HC_{coal\_res}} \quad (6)$$

$$\Delta Carbon_{RES-GAS} = \frac{\left[\left(CD_{RES\_GAS} \times HC_{coal\_res} \times EC_{coal}\right) - \sum_i Heat_i \times EC_{NG}\right]}{10^9} \quad (7)$$

RES-ELEC scenario: Carbon dioxide emissions in the RES-ELEC scenario increase because household electric heaters are less efficient than small household coal stoves.

$$CD_{RES-ELEC} = \frac{\sum_i Elec_i \times (1-\rho_{T\&D\ loss}) \times 3412 \times \eta_{elec}}{\eta_{coal} \times HC_{coal\_res}} \quad (8)$$

$$\Delta Carbon_{RES-ELEC} = \frac{\left[\left(CD_{RES-ELEC} \times HC_{coal\_res} \times EC_{coal}\right) - \sum_i Elec_i \times EF_{NG}\right]}{10^9} \quad (9)$$

S2.4 Equations for coal-fired power plant displacement in the *POW* scenarios

We determine the most polluting, existing coal power plants (CPPs) in 13 northern provinces and replace those plants with electricity generated from CBM/CMM in the POW scenario. We identify model grid boxes with coal electricity generation in the Global Power Emissions Database (GPED) [1] that have the highest effective emission factors. We use the following equation to order GPED model grid boxes from highest to lowest effective emissions factor:

$$EF_{eff,i} = \frac{E_{SO_2,i}}{E_{CO_2,i}} + \frac{E_{NOx,i}}{E_{CO_2,i}} \quad (10)$$

We displace coal power production from the grid boxes from highest to lowest effective emissions factor with CBM/CMM-generated electricity until we have depleted all available CBM/CMM for the given province.

S2.5 Coal home heating displacement in the RES-GAS and RES-ELEC scenarios

The MEIC inventory provides an estimate of overall residential emissions but not heating specific emissions. However, we can approximate home heating emissions by examining the differences between summer and winter residential emissions. We first calculate the difference between residential emissions in each month that would have home heating activities (October, November, December, January, February, and March) and average residential emissions in June and July. This setup assumes the difference in residential emissions between summer and winter months is due to home heating. Other types of residential emissions (i.e., cooking) are unlikely to vary seasonally, and seasonal differences in residential emissions are likely a good proxy for home heating. Subsequently, we reduce overall residential heating emissions in each province proportional to the amount of heating that can be supplied with available CBM/CMM resources in each province (Table S3).

Table S3. Displaced home heating-related emissions by province in the RES-GAS and RES-ELEC scenarios

Province	Removed heating-related emissions during heating season (%)			
	2020FYP		2020NEA	
	RES-GAS	RES-ELEC	RES-GAS	RES-ELEC
Shanxi	100%	66%	100%	100%
Henan	61%	3%	100%	41%
Anhui	13%	6%	11%	5%
Heilongjiang	1%	-	33%	-
Liaoning	2%	1%	3%	2%
Shaanxi	4%	2%	35%	16%
Inner-Mongolia	1%	-	17%	8%
Gansu	2%	1%	2%	1%

S3 Description of the GEOS-Chem model and the simulated $PM_{2.5}$ in base case and each utilization scenario

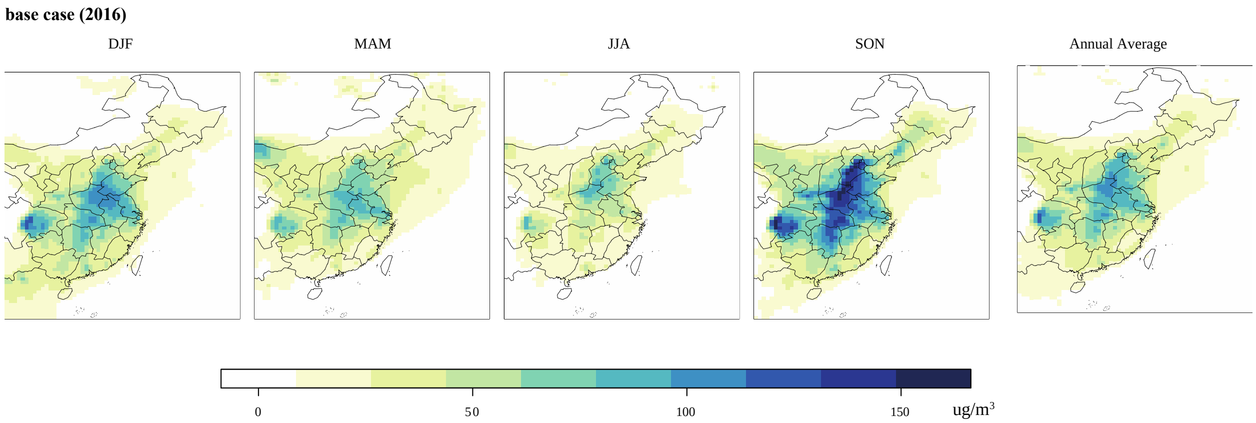

Figure S1. 2016 base case seasonal and annual mean surface $PM_{2.5}$ concentrations (unit: μg/m^3). $PM_{2.5}$ concentrations are typically higher in northern and south-central China than in more sparsely populated regions of the country.

Figure S2. Seasonal averaged $PM_{2.5}$ reduction (unit: μg/m^3) in the 2020FYP set. (Note: the two residential scenarios share one legend.)

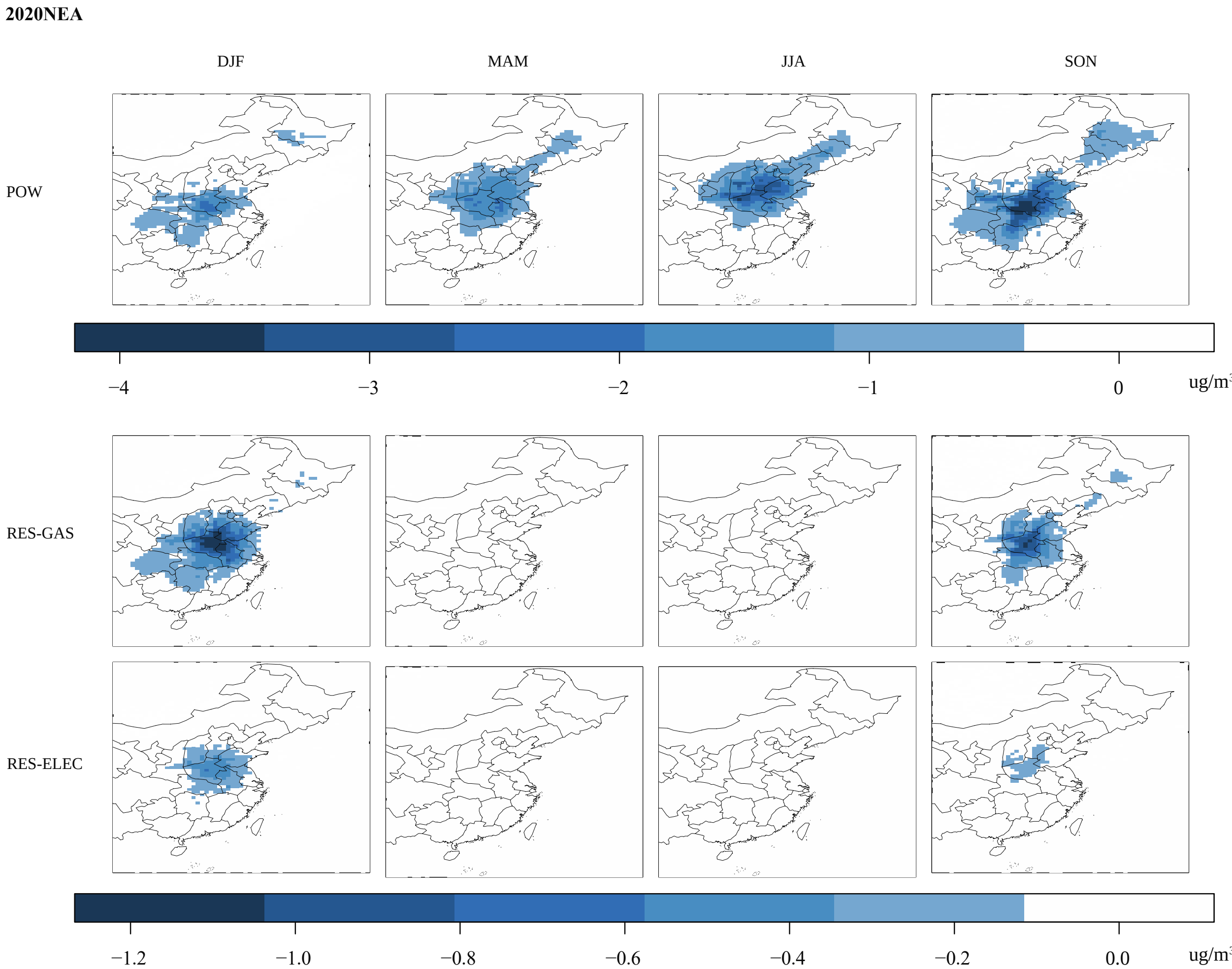

Figure S3. Seasonal averaged $PM_{2.5}$ reduction (unit: $\mu g/m^3$) in the 2020NEA set. (Note: the two residential scenarios share one legend.)

We use nested GEOS-Chem simulations to estimate surface-level ambient $PM_{2.5}$ concentrations for each scenario. We first create global GEOS-Chem simulations at a relatively coarse 4° latitude by 5° longitude resolution and use these global simulations as a boundary condition for nested East Asia simulations at a much higher resolution of 0.5° latitude by 0.625° longitude. Note that we spin up the model for two months to create initial conditions for both the global and nested East Asia grids, similar to existing GEOS-Chem studies for the East Asia model domain[6]. Both global and nested simulations are driven by assimilated meteorology from NASA's

MERRA-2 (Modern-Era Retrospective analysis for Research and Applications, Version 2)[9]. In addition, the simulations in this study have a 5-minute dynamical timestep and 10-minute chemistry timestep for multiple emission species and aerosols. The lowest vertical level in the model is approximately 100-m high and is used to represent the surface $PM_{2.5}$ concentrations in this study. We subsequently use monthly-averaged surface $PM_{2.5}$ estimated by GEOS-Chem for the health impact analysis (Sect. S10).

GEOS-Chem simulations over China have been evaluated by several existing studies. Wang et al.,2013,2014[10,11]; Lou et al.,2014[12]; and Wang et al., 2013[10] indicated that the GEOS-Chem model performed well in simulating sulfate distributions and concentrations. Wang et al.,2014[11] further evaluated the model performance in reproducing the concentrations and the spatiotemporal patterns of $PM_{2.5}$ over China during a severely polluted month in January 2013. The model shows a good correlation with $PM_{2.5}$ spatial distribution and concentration with observation, and only underestimated the concentrations of $PM_{2.5}$ and sulfate over northern China during a severe haze period (> 500 $\mu g/m^3$). In this study, we used emissions data (MEIC) for the year 2016, and the data show that the NOx and SO_2 emissions have dramatically decreased from 2012 to 2016 by 70% and 50%, respectively. Thus, combining with the results from other studies above, we believe that the GEOS-Chem model performs well in simulating the spatial distribution and concentration level of $PM_{2.5}$ over China using the anthropogenic emission data for the year 2016.

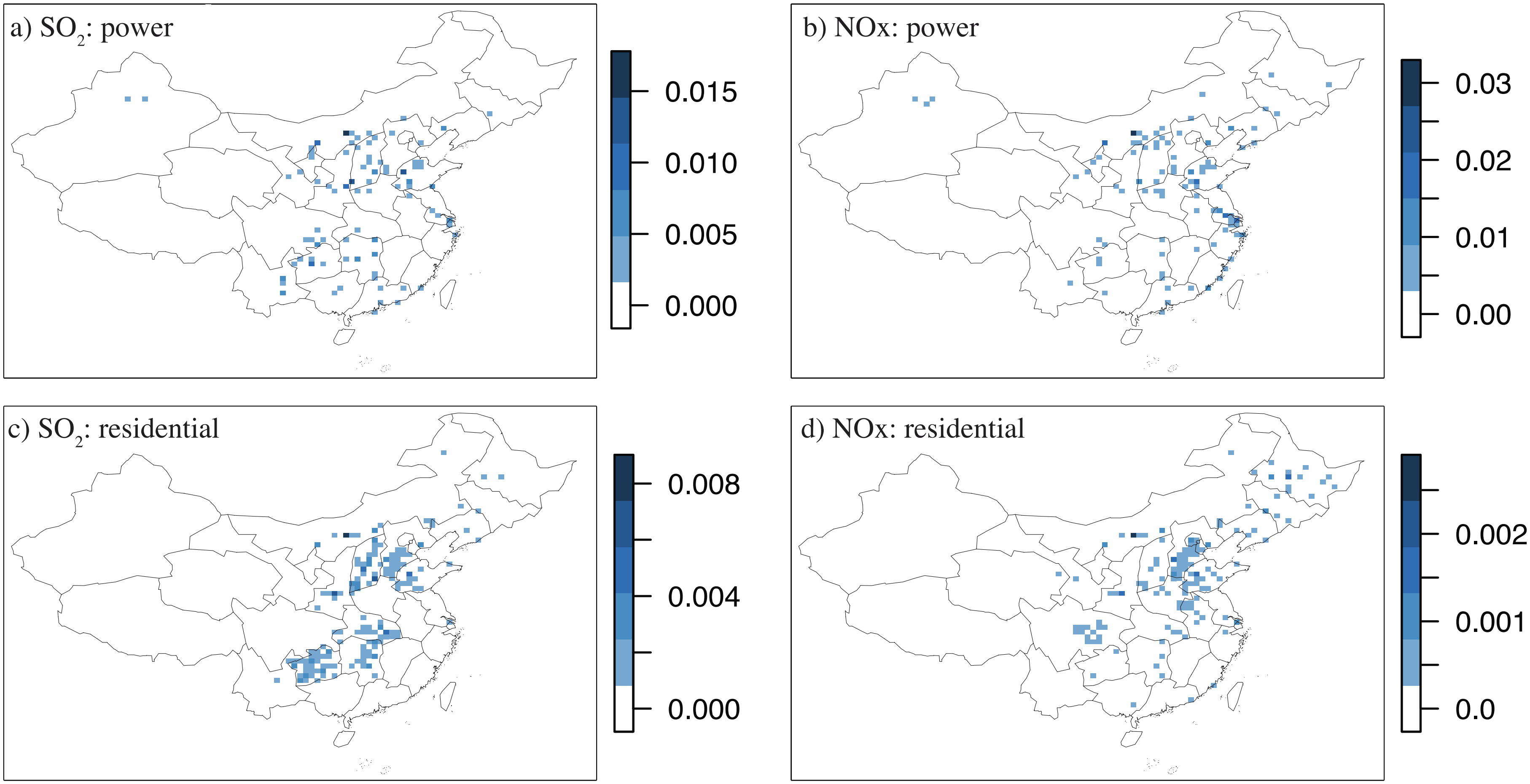

Figure S4. Gridded annual 2016 NO_x and SO_2 emissions in the base case power sector and residential sector (Unit: kg/m^2 yr). The NO_x and SO_2 emissions data are from MEIC inventory for the year 2016.

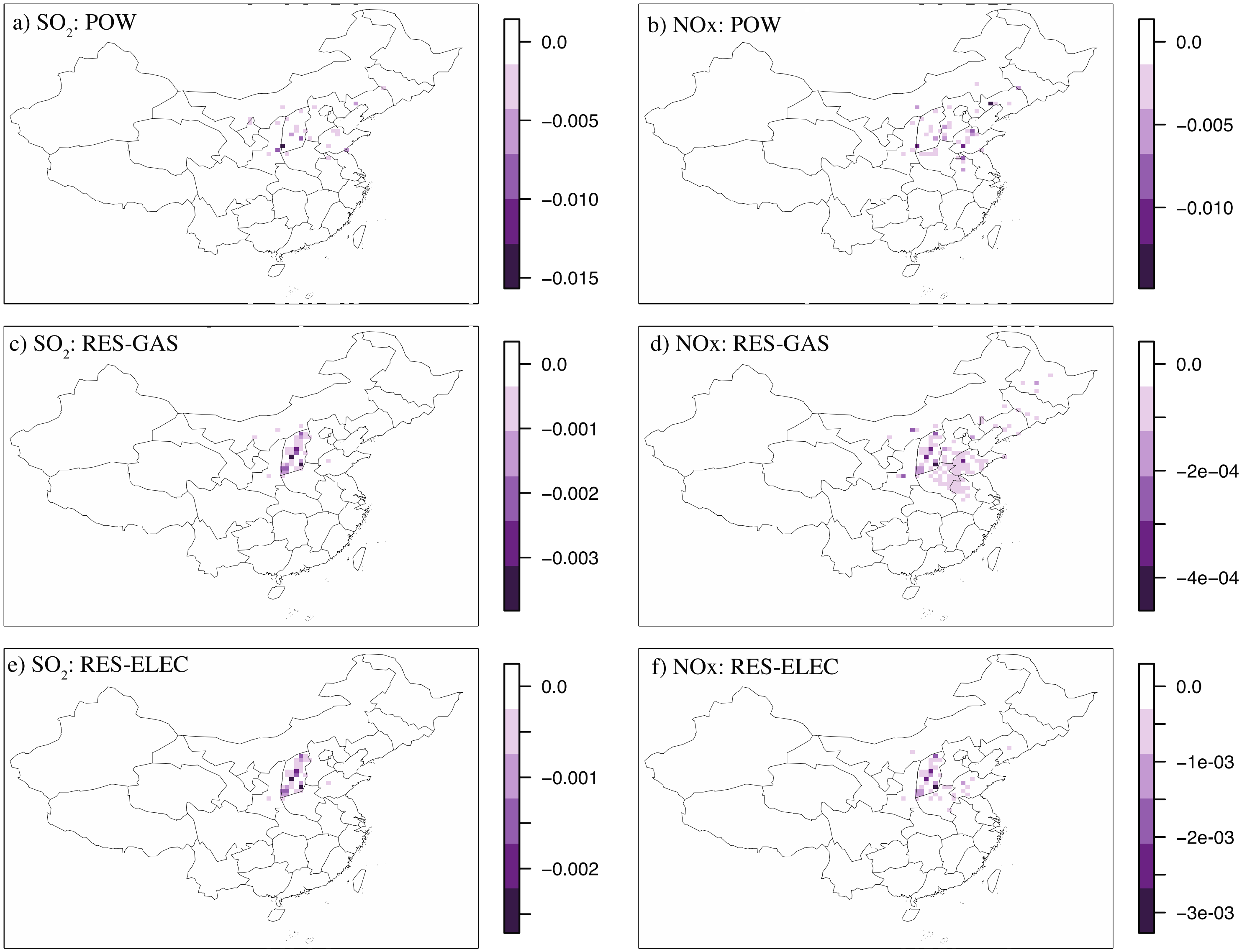

Figure S5. Gridded annual 2016 NO_X and SO_2 emission reductions in each 2020NEA scenario (Unit: kg/m^2 yr).

S4 Analysis of health impacts

We calculate reduced mortality by province from air quality changes resulting from each scenario using the following equation from the Global Burden of Disease (GBD) study[13]:

$$\Delta Mortality_{d,i} = MR_{d,base} \times POP_i \times \left(\frac{RR_{d,i}(C_s)}{RR_{d,i}(C_{base})} - 1\right) \quad (12)$$

Table S4. Summary of data for health impacts analysis

Variables	Definition	Data source
$MR_{d,\ base}$	Baseline mortality for a disease (*d*) in the total adult population	[13]
Pop_i	Adult population aged 25 and above in each province *i* in	[4]
$RR_{d,i}\ (C_s)$ and $RR_{d,i}\ (C_{base})$:	Relative risks (RR) of disease *d* in province *i* for the adult population at the $PM_{2.5}$ levels of C_s in scenario s and C_{base} in the base case, respectively.	[13]
C_s and C_{base}	Annual mean exposures in scenario *s* and the base case. This exposure is given by the 12-month average of the population-weighted, province-averaged $PM_{2.5}$ concentrations.	GEOS-Chem simulations

Note: We use RR functions from the Global Burden of Disease study[13], and the concave relative risk functions are used in the main results.

First, we estimate county-averaged $PM_{2.5}$ concentrations by averaging the concentrations for all the GEOS-Chem grids located within that county. Second, we calculate population-weighted, provincial-averaged $PM_{2.5}$ concentrations by weighting the $PM_{2.5}$ concentrations for each county within that province by the ratio of county total population to provincial total population. The county-level age and spatial distributions of the population within each province are from the 2010 China county-level census data[14].

For household indoor air pollution, we also use equation 12 but in a simplified form. The average user of solid fuels for cooking/heating is exposed to indoor $PM_{2.5}$ concentrations of 300 $\mu g/m^3$ for traditional coal stoves, and 70 for modern stoves.[15,16] We then use these two numbers to derive the relevant risk for each scenarios and diseases. The exposed population is given by the number of people using coal for home heating in the base case and each utilization scenario.

We also calculate the uncertainty range (95% confidence interval (CI)) of avoided mortalities for each scenario using the GBD model, and that model includes a relative risk function and CI for each disease. Our uncertainty ranges are asymmetrical because the CIs on each relative risk function provided by the GBD is asymmetrical. Furthermore, the $PM_{2.5}$ model outputs are treated as deterministic because GOES-Chem does not provide any uncertainty bound on the $PM_{2.5}$ model output. Thus, our uncertainty range do not include the uncertainty of GEOS-Chem modeled $PM_{2.5.}$

REFERENCES

(1) Tong, D.; Zhang, Q.; Davis, S. J.; Liu, F.; Zheng, B.; Geng, G.; Xue, T.; Li, M.; Hong, C.; Lu, Z.; Streets, D. G.; Guan, D.; He, K. Targeted emission reductions from global super-polluting power plant units. *Nature Sustainability* **2018**, *1* (1), 59–68.

(2) *Carbon Dioxide Emissions Coefficients;* U.S. Energy Information Administration, 2016; https://www.eia.gov/environment/emissions/co2_vol_mass.php.

(3) Climate change 2013: The physical science basis; Stocker, T. F.; Qin, D.; Plattner, G. K.; Tignor, M.; Allen, S. K., 2013; http://www.climatechange2013.org/images/report/WG1AR5_Frontmatter_FINAL.pdf.

(4) *China statistical yearbook (2018)*; National Bureau of Statistics of China, 2018; http://www.stats.gov.cn/tjsj/ndsj/2018/indexeh.htm.

(5) *Electric Power Annual (2019)*; U.S. Energy Information Administration, 2019; https://www.eia.gov/electricity/annual/customersales-map3.php

(6) *International Energy Outlook 2016*; U.S.Energy Information Administration (EIA), 2017; https://www.eia.gov/outlooks/ieo/pdf/0484(2016).pdf.

(7) Ding, Y.; Han, W.; Chai, Q.; Yang, S.; Shen, W. Coal-based synthetic natural gas (SNG): A solution to China's energy security and CO2 reduction? *Energy Policy* **2013**, *55*, 445–453.

(8) *Annual Statistics of China Power Industry 2015*; China Electricity Council Development and Planning Department, 2016.

(9) Gelaro, R.; McCarty, W.; Suárez, M. J.; Todling, R.; Molod, A.; Takacs, L.; Randles, C. A.; Darmenov, A.; Bosilovich, M. G.; Reichle, R.; Wargan, K.; Coy, L.; Cullather, R.; Draper, C.;

Akella, S.; Buchard, V.; Conaty, A.; da Silva, A. M.; Gu, W.; Kim, G.-K.; Koster, R.; Lucchesi, R.; Merkova, D.; Nielsen, J. E.; Partyka, G.; Pawson, S.; Putman, W.; Rienecker, M.; Schubert, S. D.; Sienkiewicz, M.; Gelaro, R.; McCarty, W.; Suárez, M. J.; Todling, R.; Molod, A.; Takacs, L.; Randles, C. A.; Darmenov, A.; Bosilovich, M. G.; Reichle, R.; Wargan, K.; Coy, L.; Cullather, R.; Draper, C.; Akella, S.; Buchard, V.; Conaty, A.; da Silva, A. M.; Gu, W.; Kim, G.-K.; Koster, R.; Lucchesi, R.; Merkova, D.; Nielsen, J. E.; Partyka, G.; Pawson, S.; Putman, W.; Rienecker, M.; Schubert, S. D.; Sienkiewicz, M.; B, Zhao. The Modern-Era Retrospective Analysis for Research and Applications, Version 2 (MERRA-2). *Journal of Climate* **2017**, *30* (14), 5419–5454.

(10) Wang, Y.; Zhang, Q. Q.; He, K.; Zhang, Q.; Chai, L. Sulfate-nitrate-ammonium aerosols over China: response to 2000–2015 emission changes of sulfur dioxide, nitrogen oxides, and ammonia. *Atmospheric Chemistry and Physics* **2013**, *13* (5), 2635–2652.

(11) Wang, Y.; Zhang, Q.; Jiang, J.; Zhou, W.; Wang, B.; He, K.; Duan, F.; Zhang, Q.; Philip, S.; Xie, Y. Enhanced sulfate formation during China's severe winter haze episode in January 2013 missing from current models. *Journal of Geophysical Research: Atmospheres* **2014**, *119* (17), 10, 425–10, 440.

(12) Lou, S.; Liao, H.; Zhu, B. Impacts of aerosols on surface-layer ozone concentrations in China through heterogeneous reactions and changes in photolysis rates. *Atmospheric Environment* **2014**, *85*, 123–138.

(13) Burnett, R.; Chen, H.; Szyszkowicz, M.; Fann, N.; Hubbell, B.; Pope, C. A.; Apte, J. S.; Brauer, M.; Cohen, A.; Weichenthal, S.; Coggins, J.; Di, Q.; Brunekreef, B.; Frostad, J.; Lim, S. S.; Kan, H.; Walker, K. D.; Thurston, G. D.; Hayes, R. B.; Lim, C. C.; Turner, M. C.; Jerrett, M.; Krewski, D.; Gapstur, S. M.; Diver, W. R.; Ostro, B.; Goldberg, D.; Crouse, D. L.; Martin, R. V.;

Peters, P.; Pinault, L.; Tjepkema, M.; van Donkelaar, A.; Villeneuve, P. J.; Miller, A. B.; Yin, P.; Zhou, M.; Wang, L.; Janssen, N. A. H.; Marra, M.; Atkinson, R. W.; Tsang, H.; Thach, T. Q.; Cannon, J. B.; Allen, R. T.; Hart, J. E.; Laden, F.; Cesaroni, G.; Forastiere, F.; Weinmayr, G.; Jaensch, A.; Nagel, G.; Concin, H.; Spadaro, J. V. Global estimates of mortality associated with long-term exposure to outdoor fine particulate matter. *Proc. Natl. Acad. Sci. USA* **2018**, *115* (38), 9592–9597.

(14) *China census data by county, 2000-2010;* All China Marketing Research Co. Ltd., 2014; https://chinadatacenter.net/Data/ServiceContent.aspx?id=1620.

(15) Balakrishnan, K.; Ghosh, S.; Ganguli, B.; Sambandam, S.; Bruce, N.; Barnes, D. F.; Smith, K. R. State and national household concentrations of PM 2.5 from solid cookfuel use: Results from measurements and modeling in India for estimation of the global burden of disease. *Environ Health* **2013**, *12* (1), 1–14.

(16) Larsen, B.; Holland, M.; Jeuland, M. Benefits and Costs of the Air Pollution Targets for the Post-2015 Development Agenda, **2014**. https://ssrn.com/abstract=2685661.